

The Interaction of Na⁺ and K⁺ in Voltage-gated Potassium Channels

Evidence for Cation Binding Sites of Different Affinity

LASZLO KISS, DAVID IMMKE, JOSEPH LOTURCO, and STEPHEN J. KORN

From the Department of Physiology and Neurobiology, University of Connecticut, Storrs, Connecticut 06269

ABSTRACT Voltage-gated potassium (K⁺) channels are multi-ion pores. Recent studies suggest that, similar to calcium channels, competition between ionic species for intrapore binding sites may contribute to ionic selectivity in at least some K⁺ channels. Molecular studies suggest that a putative constricted region of the pore, which is presumably the site of selectivity, may be as short as one ionic diameter in length. Taken together, these results suggest that selectivity may occur at just a single binding site in the pore. We are studying a chimeric K⁺ channel that is highly selective for K⁺ over Na⁺ in physiological solutions, but conducts Na⁺ in the absence of K⁺. Na⁺ and K⁺ currents both display slow (C-type) inactivation, but had markedly different inactivation and deactivation kinetics; Na⁺ currents inactivated more rapidly and deactivated more slowly than K⁺ currents. Currents carried by 160 mM Na⁺ were inhibited by external K⁺ with an apparent IC₅₀ <30 μM. K⁺ also altered both inactivation and deactivation kinetics of Na⁺ currents at these low concentrations. In the complementary experiment, currents carried by 3 mM K⁺ were inhibited by external Na⁺, with an apparent IC₅₀ of ~100 mM. In contrast to the effects of low [K⁺] on Na⁺ current kinetics, Na⁺ did not affect K⁺ current kinetics, even at concentrations that inhibited K⁺ currents by 40–50%. These data suggest that Na⁺ block of K⁺ currents did not involve displacement of K⁺ from the high affinity site involved in gating kinetics. We present a model that describes the permeation pathway as a single high affinity, cation-selective binding site, flanked by low affinity, nonselective sites. This model quantitatively predicts the anomalous mole fraction behavior observed in two different K⁺ channels, differential K⁺ and Na⁺ conductance, and the concentration dependence of K⁺ block of Na⁺ currents and Na⁺ block of K⁺ currents. Based on our results, we hypothesize that the permeation pathway contains a single high affinity binding site, where selectivity and ionic modulation of gating occur.

KEY WORDS: K⁺ channel • permeation • binding sites • selectivity

INTRODUCTION

Voltage-gated potassium channels are multi-ion, single file pores (Hodgkin and Keynes, 1955; Hille and Schwarz, 1978; Stampe and Begegnisich, 1996). Flux ratio experiments suggest that normally conducting K⁺ channels are occupied by three to four K⁺ ions simultaneously (Hodgkin and Keynes, 1955; Stampe and Begegnisich, 1996), and studies of Ba²⁺ lock-in and enhancement provided evidence for the existence of three to four different K⁺ binding sites in Ca²⁺-dependent K⁺ channels (Neyton and Miller, 1988). In the face of essentially equal concentration gradients for K⁺ and Na⁺, voltage-gated K⁺ channels are highly selective for K⁺ over Na⁺, with permeability ratios ~100:1 (Hille, 1992). Indeed, Na⁺ has rarely been observed to conduct through K⁺ channels at all, except under extreme voltages (French and Wells, 1977).

The most widely accepted theory to explain ionic selectivity in K⁺ channels is embodied in the “close-fit”

hypothesis (Bezanilla and Armstrong, 1972; Hille, 1973; Armstrong, 1989). This hypothesis postulates that the channel pore is lined with negatively charged groups that form “binding sites.” One of the intrapore binding sites is thought to be associated with a narrow constriction, which forms the selectivity filter. In the hydrated state, ions are too large to fit through the narrow constriction, so that to traverse the channel, ions must lose waters of hydration. The energy needed to dehydrate the ions is provided by the formation of bonds between the ions and the binding sites in the pore wall, with the last dehydration step occurring at the selectivity filter. The hypothesis postulates that Na⁺ and Li⁺ are too small to fit closely into the narrow region, and thus cannot sufficiently dehydrate to pass through. Larger ions (i.e., Cs⁺) are too large to pass through the constriction. Thus, this model postulates that selectivity is accomplished by a sieve-like exclusion mechanism, based on both ionic radius (for larger ions) and thermodynamic factors (for smaller ions).

An enduring feature of Hodgkin and Keynes’ (1955) original model of a multi-ion pore is the concept that all K⁺ binding sites in the channel are more or less alike. Thus, the multiple K⁺ binding sites in K⁺ channel pores have generally been considered to have ap-

Address correspondence to Dr. Stephen Korn, Department of Physiology and Neurobiology, Box U-156, University of Connecticut, 3107 Horsebarn Hill Rd., Storrs, CT 06269. Fax: 860-486-3303; E-mail: korn@oracle.pnb.uconn.edu

proximately equal affinities (Begenisich and Smith, 1984; French and Shoukimas, 1985; Neyton and Miller, 1988; Perez-Cornejo and Begenisich, 1994). However, K^+ binds with very high affinity to at least some binding sites in the pore (Yellen, 1984; French and Shoukimas, 1985; Neyton and Miller, 1988). To reconcile the high flux rates through pores with the presence of multiple high affinity binding sites, it is generally postulated that multiple ions packed closely together in the pore electrostatically repel each other (Hille and Schwarz, 1978; Almers et al., 1984; Hess and Tsien, 1984; Yellen, 1984). This repulsion in multiply occupied channels results in an effective lowering of the affinity for the ions in the pore (French and Shoukimas, 1985; Neyton and Miller, 1988; Shumaker and MacKinnon, 1990; Perez-Cornejo and Begenisich, 1994). However, the most detailed studies of intrapore K^+ binding sites that were interpreted in this way (Neyton and Miller, 1988) are also consistent with the hypothesis that sites have different binding affinities that range from tens of micromolar to hundreds of millimolar. Furthermore, molecular studies suggest that the conduction pathway consists of a very short constricted region flanked by a wide outer and inner vestibules (Hidalgo and MacKinnon, 1995; Goldstein, 1996; Miller, 1996; Ranganathan et al., 1996; Holmgren et al., 1997). These observations do not fit well with the picture of a long, narrow region with identical cation binding sites.

Ca^{2+} channels represent another class of voltage-gated, multi-ion pores. Ca^{2+} channels are highly selective for Ca^{2+} in the presence of Ca^{2+} , but allow monovalent cations to permeate well in the absence of Ca^{2+} . Addition of low $[Ca^{2+}]$ inhibits monovalent ion flux through Ca^{2+} channels, and further elevation of Ca^{2+} produces Ca^{2+} currents. As in K^+ channels, multiple binding sites within the Ca^{2+} channel pore were classically considered to have identical binding affinities, which were effectively lowered due to electrostatic repulsion between ions when the pore was multiply occupied (Almers et al., 1984; Hess and Tsien, 1984). However, molecular studies suggest that Ca^{2+} channels contain only a single high affinity binding site for Ca^{2+} (Kim et al., 1993; Yang et al., 1993; Ellinor et al., 1995). Furthermore, high external concentrations of monovalent cations compete with Ca^{2+} for entry into a pore that already has a high affinity site saturated by Ca^{2+} (Kuo and Hess, 1993; Polo-Parada and Korn, 1997). This is consistent with the presence of a low affinity binding site external to a high affinity site in the channel. Recently, Dang and McCleskey (1996) showed that Ca^{2+} channels need not contain two high affinity binding sites to produce their observed permeation properties. Rather, a pore that contains a single high affinity binding site, flanked by low affinity binding sites, could account well for anomalous mole fraction behavior, the

high degree of selectivity, and the high flux rate of Ca^{2+} channels. No electrostatic repulsion was necessary, and binding sites had stable affinities regardless of pore occupancy.

Recently, we demonstrated that in at least one cloned K^+ channel, Kv2.1, competition between K^+ and Na^+ contributes to the mechanism of selectivity (Korn and Ikeda, 1995). Indeed, the permeation mechanism in Kv2.1 appears to be quite similar to that of Ca^{2+} channels. Kv2.1 is highly selective for K^+ in the presence of K^+ , and upon removal of K^+ , Na^+ , Li^+ , and Cs^+ conduct well (Korn and Ikeda, 1995; Immke, D., L. Kiss, J. Lo-Turco, and S.J. Korn, manuscript in preparation). Addition of relatively low concentrations of K^+ inhibited permeation of these other cations through Kv2.1, and further elevation of $[K^+]$ resulted in the production of K^+ currents.

In this paper, we present evidence that ionic selectivity and multi-ion behavior in K^+ channels may reflect permeation through a pore that contains a single high affinity binding site, flanked by low affinity, nonselective cation binding sites. These binding sites may have a fixed affinity regardless of channel occupancy, and a high flux rate through channels does not require electrostatic repulsion between ions. The hypothesis we present about the nature of the permeation pathway not only accounts for much of the observed behavior of at least two K^+ channels, but also makes predictions about the site of K^+ -dependent influences on channel gating.

METHODS

Cell Culture and Channel Expression

K^+ channel cDNA was subcloned into the pcDNA3 expression vector. Channels were expressed in the human embryonic kidney cell line, HEK293 (American Type Culture Collection, Rockville, MD), maintained in culture in a $37^\circ C$, 5% CO_2 incubator, in DMEM plus 10% fetal bovine serum with 1% penicillin/streptomycin (maintenance media). Cells (40–70% confluent) were split 2 d before transfection by incubation with 0.05% trypsin in Ca^{2+} -free, Mg^{2+} -free Hanks balanced salt solution. After trypsinization, cells were washed and resuspended in HEPES-buffered saline (160 mM NaCl, 25 mM HEPES, 1.6 mM $NaHPO_4$, pH 7.3, osmolality 293) and either replated for later use or used for transfection.

Cells (2×10^6 cells/ml) were cotransfected by electroporation (71 μF , 375 V, Electroporator II; Invitrogen Corp., San Diego, CA) with channel expression plasmid (15 $\mu g/0.2$ ml) and the CD8 antigen (3 $\mu g/0.2$ ml). After electroporation, cells were plated on protamine (1 mg/ml; Sigma Chemical Co., St. Louis, MO)-coated glass cover slips submerged in maintenance media. Electrophysiological recordings were made 18–30 h later. On the day of recording, cells were washed with fresh media and incubated with Dynabeads M450 conjugated with antibody for CD8 (1 $\mu l/ml$; Dynal, Oslo, Norway). The beads preferentially bind to cells expressing CD8, and thus allow visualization of transfected cells (Jurman et al., 1994). More than 90% of cells expressing CD8 also expressed K^+ channels. Untransfected cells displayed no time-dependent currents.

Data are presented from two channels. DRK1 was obtained from Dr. Christopher Miller (Brandeis University, Waltham, MA). We also used a chimeric channel that originated with Dr. Rod MacKinnon (Rockefeller University, New York) ("chimera," Gross et al., 1994), and was handed to us presciently by Dr. Miller. The chimeric channel consists of the P-region and P-region linkers to S5 and S6 transmembrane domains from Kv1.3 swapped into the backbone of Kv2.1 (Fig. 1 A). The differences in amino acid sequence between Kv2.1 and the chimera are shown in Fig. 1 B.

Electrophysiology

Currents were recorded using either the whole-cell patch clamp technique (Hamill et al., 1981) or the excised, outside-out patch clamp technique. Patch pipettes were fabricated from N51A glass (Garner Glass Co., Claremont, CA), coated with Sylgard and fire-polished. Series resistance ranged from 1.5 to 2.2 M Ω in whole cell experiments, and was compensated by 80–90% (Axopatch 1D; Axon Instruments, Foster City, CA). Currents were filtered at 2–5 kHz (internal Axopatch filter), sampled at 70–600 μ s/point, and evoked by depolarizing stimuli once every 5 s. The holding potential was always -80 mV and the repolarization potential was -80 mV unless otherwise noted in the figure. All summed experimental data are reported as mean \pm SEM.

Electrophysiological Solutions

Currents were recorded in a constantly flowing, gravity-fed bath. Solutions were placed in one of six reservoirs, each of which was fed via plastic tubing into a single quartz tip (~ 100 μ m diameter; ALA Scientific Instruments, Westbury, NY). This tip was placed within 10 μ m of the cell being recorded before the start of the experiment. One solution was always flowing, and solutions were changed by manual switching (complete solution changes took 5–10 s). Internal solutions contained (mM): 140 XCl (X = K $^+$, Na $^+$, or Tris $^+$), 20 HEPES, 10 EGTA, 1 CaCl $_2$, 4 MgCl $_2$, pH 7.3 (with *N*-methyl-D-glucamine), osmolality 285. External solutions always contained (mM): 20 HEPES, 10 glucose, 2 CaCl $_2$, 1 MgCl $_2$, pH 7.3, osmolality 320. Cationic additions to this basic external solution are listed in the figure legends.

NaCl (99.99%, cat. #87605; Alfa Aesar, Ward Hill, MA) was used in most Na $^+$ -containing solutions. Contaminating [K $^+$] in external solutions that contained 150 mM NaCl was <14 μ M (measured by flame photometry at the University of Connecticut Biotechnology Center, Storrs, CT). Higher purity NaCl (99.999%, cat. #10862; Alfa Aesar), which produced external solutions with <4 μ M contaminating K $^+$, was used in some experiments and gave apparently identical results.

The Permeation Model

We used a computer simulation, described in detail in Dang and McClesley (1998), to model the permeation pathway. Briefly, the

model consists of four barriers and three wells. Each well can be empty or occupied by either of two ions. Consequently, at any given voltage and any set of ion concentrations, the channel can be in 1 of 27 possible states. Model parameters are listed in the figure legends.

RESULTS

Anomalous Mole Fraction Behavior in the Chimera

Fig. 2 illustrates chimeric currents carried by K $^+$ and Na $^+$. In the presence of internal K $^+$ and external Na $^+$, depolarizations evoked sustained outward K $^+$ currents (Fig. 2, A and B). Upon repolarization to -80 mV, the chimera displayed outward K $^+$ currents, which illustrates that the channel is highly selective for K $^+$. As with one of the parent channels, Kv2.1, the chimera conducted Na $^+$ in the absence of internal and external K $^+$ (Fig. 2, C and D). Currents carried by Na $^+$ and K $^+$ activated with identical voltage dependence ($V_{1/2} = -4.66 \pm 3.5$ mV, $n = 8$, and -1.0 ± 2.1 mV, $n = 6$, respectively), and Na $^+$ currents reversed at the Na $^+$ equilibrium potential (Fig. 2 D). Inactivation kinetics differed markedly when chimeric currents were carried by Na $^+$ and K $^+$, and will be discussed in detail elsewhere. Of relevance to this paper, however, is the observation that inactivation of K $^+$ currents was much slower than inactivation of Na $^+$ currents.

In Kv2.1, Na $^+$ currents are inhibited by addition of low concentrations of K $^+$ (Korn and Ikeda, 1995). We tested the chimera to determine whether it showed similar competition between K $^+$ and Na $^+$. The first trace in Fig. 3 A illustrates an inward Na $^+$ current through the chimera recorded in the absence of K $^+$. External addition of K $^+$ at a concentration as low as 0.03 mM inhibited the Na $^+$ current (Fig. 3 B; see Fig. 9 for illustration of currents). Elevation of K $^+$ above 0.3 mM resulted in an increased current magnitude due to the generation of inward K $^+$ currents (Fig. 3, A and B). Thus, like Kv2.1, the chimera displays anomalous mole fraction behavior between K $^+$ and Na $^+$. However, the chimera appears to have a markedly higher relative affinity for K $^+$ over Na $^+$ than Kv2.1. In steady state experiments similar to those described here, measurable

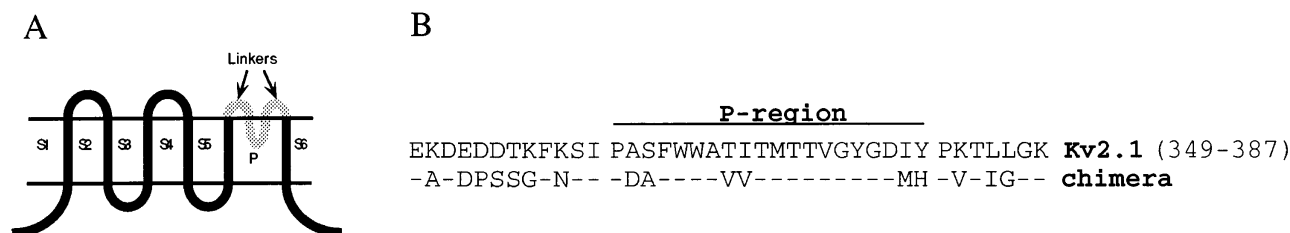


FIGURE 1. Amino acid differences between Kv2.1 and the chimera. (A) Schematic of a K $^+$ channel subunit, showing the construction of the chimera (dark region is from Kv2.1, light region is from Kv1.3). (B) Amino acid sequence of the swapped region in Kv2.1 and the chimera. The dashes denote identical residues.

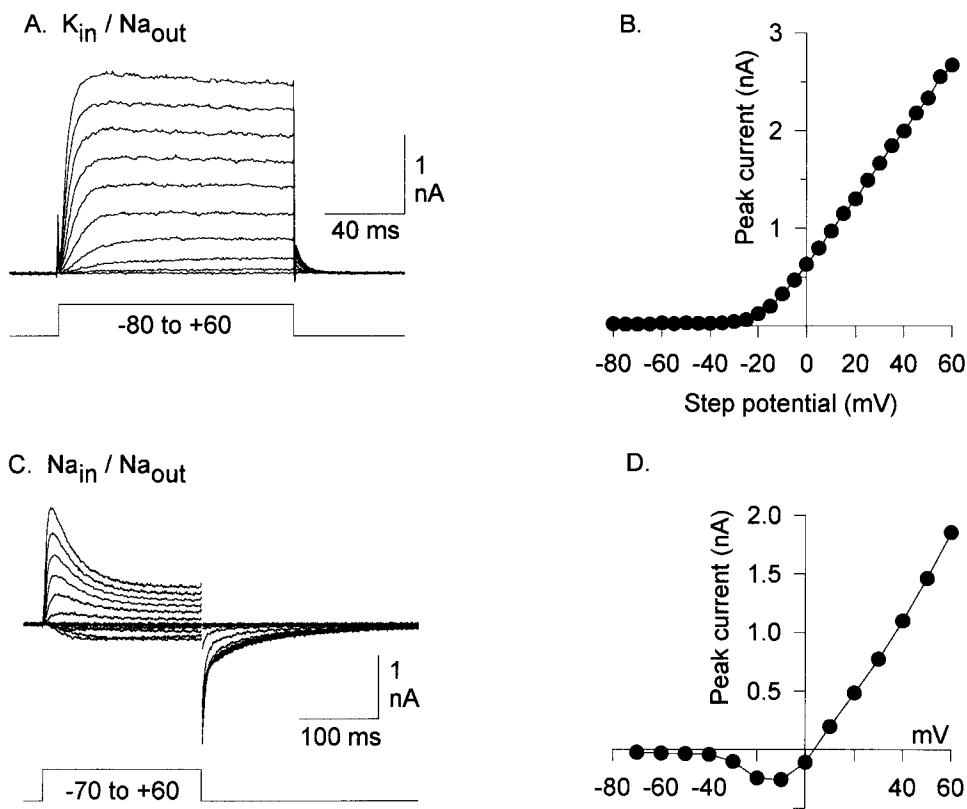


FIGURE 2. Currents through the chimera. (A) Potassium currents evoked by 120-ms depolarizing steps between -80 and $+60$ mV. The intracellular solution contained 140 mM KCl, the external solution contained 160 mM NaCl. (B) I-V relationship from currents in A. (C) Sodium currents evoked by 200-ms depolarizing steps. Solutions were identical to those in A, except that internal KCl was replaced by NaCl. (D) I-V relationship from currents in C. Currents reversed at the Na^+ equilibrium potential.

block of inward Na^+ currents through Kv2.1 required external application of 0.3 mM K^+ or more (Korn and Ikeda, 1995; see Fig. 6). In near equilibrium experiments with Kv2.1 (where Na^+ could pass unimpeded but K^+ could not traverse the channel), the IC_{50} for block of Na^+ currents by external K^+ was 0.4 mM (not shown). In contrast, the anomalous mole fraction curve in Fig. 3 B indicates that block of chimeric Na^+ currents by K^+ must occur with an $IC_{50} < 0.1$ mM and probably < 0.03 mM. These data suggest that K^+ has a very high affinity for at least one binding site in the chimera pore.

Model of the Permeation Pathway

The anomalous mole fraction behavior in the chimera indicated that K^+ binds to the pore with an affinity in the micromolar range. This observation, together with the recent demonstration by Dang and McCleskey (1996) that a single, fixed, high affinity site could account for anomalous mole fraction behavior in Ca^{2+} channels, suggested to us that K^+ channels may similarly have a single, fixed, high affinity site where this competition between K^+ and Na^+ occurs. This hypothesis is consistent with molecular studies, which suggest that the region of the pore at which selectivity occurs is very short (see Goldstein, 1996). Fig. 4 A illustrates a model that depicts this hypothesis. This model assumes three cation binding sites in the pore, only one of which has a much higher affinity for K^+ than Na^+ . This

"high affinity" site is flanked by binding sites of lower affinity, which are nearly nonselective between K^+ and Na^+ . In addition, Na^+ must overcome somewhat higher energy barriers than K^+ . Even in the absence of K^+ , Na^+ has a lower conductance than when K^+ is the charge carrier (Fig. 3 B). There is no repulsion factor in this model; the affinity of each binding site remains fixed regardless of pore occupancy.

Fig. 4 B illustrates the anomalous mole fraction curve predicted by the model in Fig. 4 A (solid line), superimposed on the experimentally determined data (symbols, taken from Fig. 3 B). These results demonstrate that this type of model can account well for anomalous mole fraction behavior in this K^+ channel.

According to this hypothesis, the block of Na^+ currents by low concentrations of K^+ occurs via a competitive interaction between K^+ and Na^+ at the high affinity binding site (described in more detail below). The outer binding site, however, would also be expected to be a site of competition between K^+ and Na^+ , since the site has nearly equal affinities for the two ions. At 3 mM K^+ , the postulated high affinity binding site is fully saturated by K^+ even in the presence of 160 mM Na^+ (described below). However, the outer binding site is nearly nonselective between K^+ and Na^+ . Consequently, the model predicts that increasing external Na^+ will reduce the entry of K^+ into the channel, and thus inhibit K^+ currents, by competition at the external low affinity site. To examine whether this predicted be-

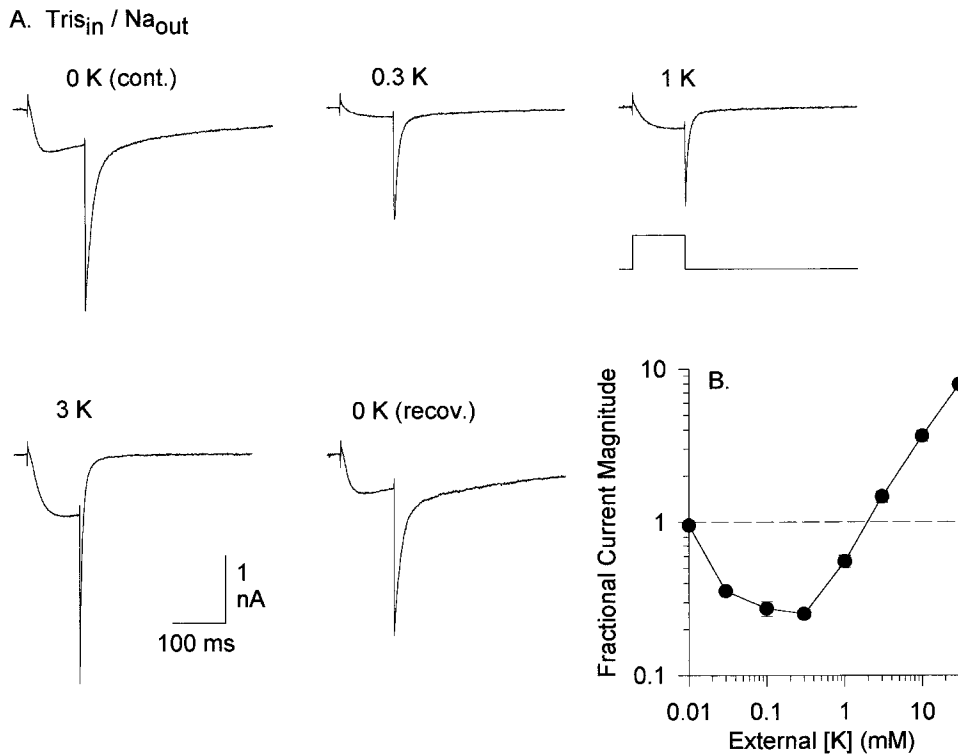


FIGURE 3. Anomalous mole fraction behavior between K^+ and Na^+ . (A) Traces were evoked by a 100-ms depolarization to 0 mV. For all traces, the internal solution contained 140 mM TrisCl and the external solution contained 160 mM NaCl. Currents were recorded in the presence of the indicated $[K^+]$ from a single cell. (B) Complete anomalous mole fraction curve; data points represent measurements from 4–12 cells. At all concentrations, external K^+ was added to the control external solution. Currents were recorded sequentially at increasing $[K^+]$, with the external solution being returned to the 0 mM K^+ solution between each application of a different $[K^+]$. Fractional current magnitude was calculated by measuring the peak inward current at 0 mV for each $[K^+]$, normalized to the current magnitude for the current evoked in 0 mM K^+ immediately preceding it.

behavior occurred experimentally, we examined Na^+ block of K^+ currents carried by a low concentration (3 mM) of K^+ (Fig. 5).

Fig. 5 A illustrates inward currents carried by 3 mM K^+ . Application of 100 mM Na^+ reversibly blocked the K^+ currents at both 0 and -60 mV. The symbols in Fig. 5 B show the results of this type of experiment with four concentrations of external Na^+ , ranging from 3 to 100 mM. Increasing $[Na^+]$ over this range produced a progressive increase in K^+ current block. Consistent with this effect occurring in the channel pore, block at -60 mV was greater than block at 0 mV for all $[Na^+]$. The solid lines illustrate the results predicted by the model in Fig. 4 A. Again, the experimental results are well-fit by the model.

The model in Fig. 4 A is also consistent with other observations made with the channel. The model predicts linear current–voltage (I–V)¹ curves $\cong 100$ mV when currents are carried by 150 mM internal and external K^+ or Na^+ , and predicts a conductance ratio, g_{Na}/g_K , of 4%. Experimentally, the chimera displays linear I–V relationships for both K^+ and Na^+ , and a conductance ratio of $\sim 2.5\%$ (data not shown).

Extension of the Model to Kv2.1

To be of value, the model should, with minor changes in parameter values, be able to account for permeation

behavior in other channels. A striking difference between Kv2.1 and the chimera is an ~ 30 -fold shift to the right of the anomalous mole fraction curve between K^+ and Na^+ (Korn and Ikeda, 1995). This is suggestive of a lower apparent affinity for K^+ relative to Na^+ at the high affinity binding site in Kv2.1. Our goal, therefore, was to determine whether the model could produce this shift with only minor adjustments to the parameters. In other words, could the model, while retaining its essential feature of a fixed high affinity binding site for K^+ flanked by low affinity, essentially nonselective cation binding sites, produce a 30-fold shift to the right in the anomalous mole fraction curve.

Fig. 6 A illustrates a model that does indeed produce this shift. Fig. 6 B shows the experimentally derived data from Kv2.1 (symbols), the predicted curve generated by the model in Fig. 6 A under the exact conditions of the experiment (solid line), and a replot of the curve predicted from the model in Fig. 4 A (dashed line). Comparison of the models in Figs. 4 A and 6 A demonstrates that the essential features of the model were retained, with minor alterations made in several parameters.

The model in Fig. 6 A differs from that in Fig. 4 A by small changes in three attributes. The affinity of the high affinity site for K^+ was reduced by 1.5 RT units (just 12%), access of Na^+ to the channel from the external side was increased by reducing the entry barrier and the outer well depth, and the overall Na^+ conductance was increased by reducing the internal energy

¹Abbreviation used in this paper: I–V, current–voltage.

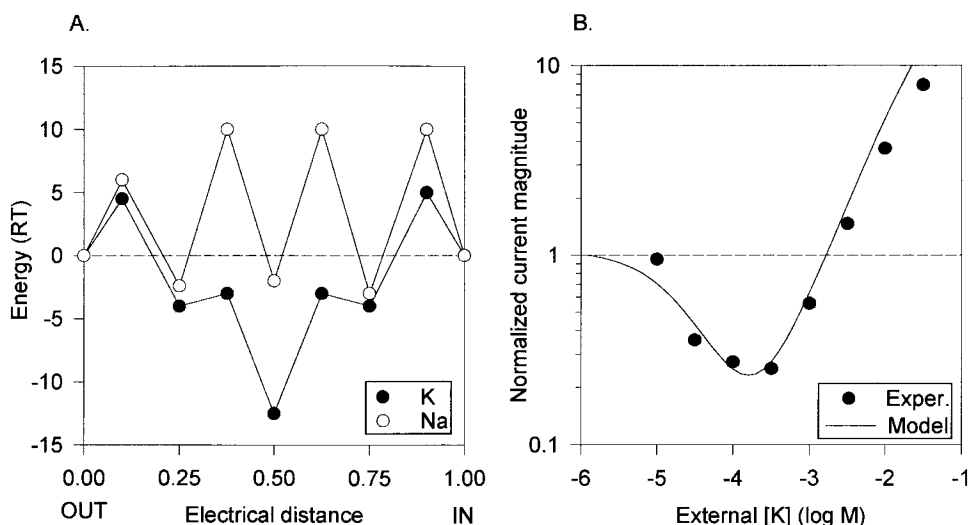


FIGURE 4. Single high affinity site model of the K⁺ channel permeation pathway. (A) Free energy diagram, illustrating ionic free energy for K⁺ (dark circles) and Na⁺ (light circles) as a function of distance in the membrane field. The central free energy well represents a high affinity binding site selective for K⁺. The wells at electrical distances of 0.25 and 0.75 are low affinity and relatively nonselective. The external solution is at electrical distance 0.00. No attempt was made to optimize placement of the wells within the field, as we do not have sufficient experimental data to do so. However, limited manipulation of distance parameters indicated that they had little

influence on the predicted results. Energy maxima for K⁺ (all values are listed from outside to inside, in RT units): 4.5, -3, -3, and 5. Energy minima for K⁺: -4, -12.5, and -4. Energy maxima for Na⁺: 6, 10, 10, and 10. Energy minima for Na⁺: -2.4, -2, and -3. (B) Predicted anomalous mole fraction curve (solid line) generated by the model in A, under the experimental conditions of Fig. 3 B. The data points are a replotting of the data in Fig. 3 B, without error bars, for comparison.

barriers to Na⁺. The model also supports other data obtained with Kv2.1. It predicts the experimentally observed linear I-V curves in equimolar concentrations of K⁺ or Na⁺, and predicts a conductance ratio within ~4% of that observed in Kv2.1 (not shown).

Demands of the Model

If the pore does, indeed, contain a single high affinity binding site with fixed affinity, then there must be low

affinity binding sites both external and internal to it. A channel with a fixed, high affinity site either at the most internal or external position would produce a strongly rectifying I-V curve in symmetric ion concentrations, with little current passing in the direction where the last site in the conduction pathway is the high affinity site (not shown). This rectification occurs because the ion needs a step-up energy transfer to exit the channel. Without this step to an intermediate affinity site, the ion cannot obtain the energy to leave the

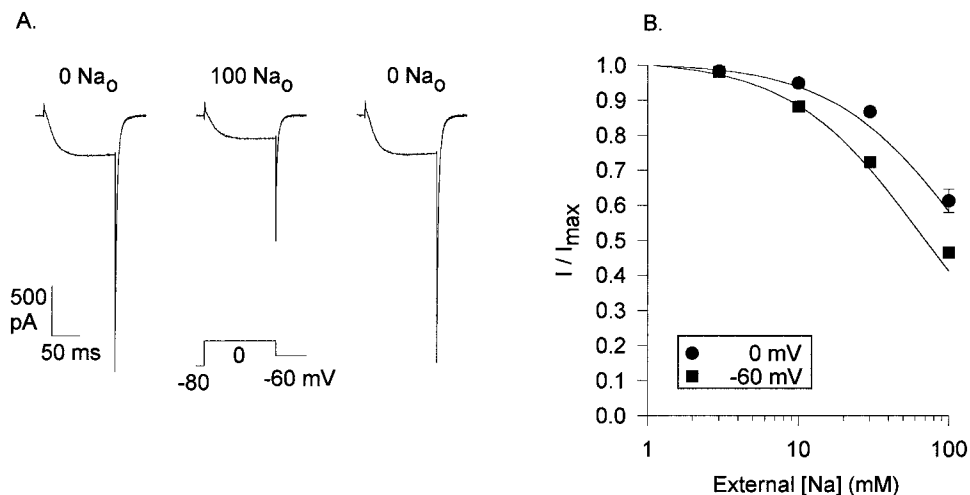


FIGURE 5. Block of inward K⁺ currents by external Na⁺. (A) Inward K⁺ currents, evoked by a 130-ms depolarization to 0 mV, in the presence and absence (control and recovery) of 100 mM external Na⁺. The external solution contained 3 mM K⁺ and 165 mM Tris⁺. The internal solution contained 140 mM Tris⁺. (B) Fractional K⁺ current as a function of external [Na⁺]. Symbols represent mean of 4–10 cells tested, with at least two Na⁺ concentrations being tested on each cell. All error bars are plotted. Peak currents were measured either at 0 mV (●) or 210 μs after repolarization to -60 mV (■; tail currents were digitized at 70 μs/point). (B, solid lines) Block of K⁺ currents by external Na⁺ under the exact conditions of these experiments, predicted by the model in Fig. 4 A.

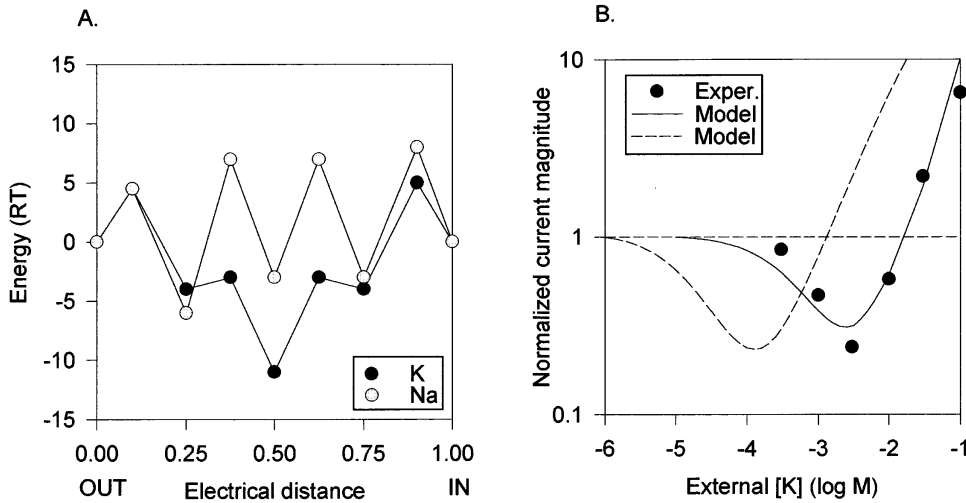


FIGURE 6. Model of Kv2.1 experimental data. (A) Free energy diagram as in Fig. 4 A, except with the following parameters: Energy maxima for K⁺: 4.5, -3, -3, and 5. Energy minima for K⁺: -4, -11, and -4. Energy maxima for Na⁺: 4.5, 7, 7, and 8. Energy minima for Na⁺: -6, -3, and -3. (B, ●) Anomalous mole fraction behavior between K⁺ and Na⁺ in Kv2.1, adapted from Korn and Ikeda (1995). (B, solid line) Anomalous mole fraction behavior predicted by the model in A, for the conditions of the experimental data collection. The curve at [K⁺] higher than 3 mM represents connected points in a discontinuous function, as the experimental data above these concentrations were collected by substituting K⁺ for equimolar concentrations of Na⁺. (B, dashed line) Replot of the predicted curve in Fig. 4 B for comparison.

high affinity site. Such rectification is not observed experimentally.

Additional Predictions of the Model

Fig. 7 illustrates the predicted steady state occupancy of the outer two binding sites by K⁺ and Na⁺ under the experimental conditions of Fig. 3. At high [Na⁺] and 0 K⁺, both the outer, low affinity site and the high affinity site are occupied by Na⁺. As very low concentrations of K⁺ (<~1 mM) are added, occupancy of the high affinity site by Na⁺ is decreased and occupancy of this site by K⁺ increases until the high affinity site is saturated by K⁺ at concentrations near 1 mM (Fig. 7 B). However, the external, nonselective site is occupied exclusively by Na⁺ until a [K⁺] of ~1 mM is reached (Fig. 7 A). Thus, this model predicts that the influence of K⁺ on channel behavior at concentrations of <1 mM results from binding to the high affinity site.

Interestingly, the model predicts that an inner binding site can be occupied without significant occupation of the outer binding site. This fits with a molecular picture of the pore having a wide outer vestibule quickly narrowing to the selectivity filter. It does not, however, violate the requirement of single file flow through the channel, since the outer site is often unoccupied, both in the steady state and transiently.

Under the experimental conditions of Fig. 5, the opposite is predicted (Fig. 8). At a concentration of 3 mM K⁺, the high affinity site is always saturated by K⁺ and never occupied by Na⁺, regardless of [Na⁺] (Fig. 8 B). As external Na⁺ is elevated, occupancy of the external,

low affinity site by Na⁺ increases and occupancy of this site by K⁺ decreases (Fig. 8 A).

One test of this hypothesis would be to demonstrate that a functional property of a pore-related channel function changed with a predicted change in occupancy of one site but not the other. For example, this hypothesis predicts that addition of low concentrations of K⁺ in the presence of high external [Na⁺] will influence a channel property associated with the high affinity binding site but not the low affinity, outer site. Conversely, in the presence of 3 mM K⁺, addition of Na⁺ will influence channel properties that are associated with the low affinity, outer site but not the high affinity site.

Cation-dependent Effects on Channel Gating

As observed in Fig. 2, slow inactivation of chimeric currents is dependent on the permeating cation. Currents carried by K⁺ inactivate very slowly (Fig. 2 A; the inactivation time constant is ~1 s; not shown), whereas currents carried by Na⁺ inactivate more rapidly (Fig. 2 C). The effects of K⁺ on inactivation can be seen more clearly in Fig. 9 A. Inward Na⁺ currents, evoked by depolarization to 0 mV in the absence of K⁺, inactivate by ~50% during a 100-ms depolarization. Addition of as little as 0.03 mM K⁺ not only blocks the current, but also virtually eliminates inactivation over this time scale. The model suggests that the high affinity site is involved in both of these K⁺-dependent effects, since at these [K⁺], K⁺ would neither bind to the external low affinity site nor reduce the occupation of Na⁺ at this

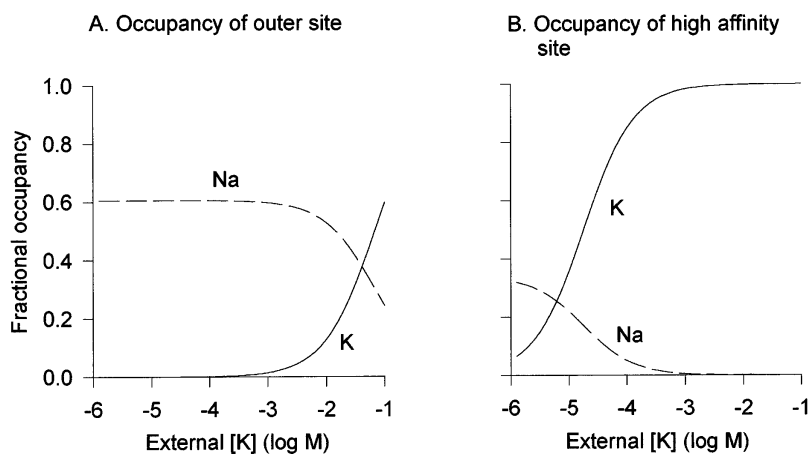


FIGURE 7. Predicted binding site occupancy with high external $[Na^+]$ and increasing external $[K^+]$. The model parameters from Fig. 4 A were used to predict the occupancy of the outermost and central, high affinity binding site at 0 mV with 160 mM external Na^+ , as a function of increasing external $[K^+]$. There was no internal K^+ or Na^+ . (A) Fractional occupancy of the outer, low affinity site by Na^+ (dashed line) and K^+ (solid line). (B) Fractional occupancy of the central, high affinity site by Na^+ (dashed line) and K^+ (solid line).

site. By definition, the block of Na^+ currents by K^+ is occurring at a "selectivity filter." Consequently, these results further suggest that the K^+ -dependent slowing of inactivation is occurring at the selectivity filter.

The rate of deactivation in the chimera was also K^+ dependent; addition of very low $[K^+]$ dramatically increased the rate of deactivation (Fig. 9 A; similar results were obtained in Kv2.1; Korn and Ikeda, 1995). This can be seen more clearly on the expanded time scale in Fig. 9 B. The rate of deactivation was slowest in the absence of K^+ . The rate of deactivation was increased by addition of 0.03 mM external K^+ , a concentration at which the high affinity site is predicted to be occupied partially by K^+ and partially by Na^+ (Fig. 7 B). At a $[K^+]$ of 10 mM, where the high affinity binding site would be occupied only by K^+ , the deactivation rate was even faster. Thus, these data suggest that the cation dependence of deactivation rate also results from the interaction of K^+ with the high affinity binding site.

The conditions of Fig. 5, where external $[Na^+]$ was increased to block K^+ currents, provides a means to examine a change in occupancy of the outer binding site. Under these conditions, the model predicts that the high affinity binding site will be occupied by K^+ regard-

less of $[Na^+]$ (Fig. 8 B). Occupancy of the external, low affinity binding site, however, is predicted to switch from predominantly K^+ to predominantly Na^+ as $[Na^+]$ is elevated (Fig. 8 A). If, indeed, the cation-dependent effects on gating kinetics occur at the high affinity and not the external, low affinity site, the model predicts that addition of Na^+ will not influence gating kinetics.

Examination of the traces in Fig. 10 provides evidence that this is indeed the case. The traces in Fig. 10 A illustrate normalized currents recorded in the presence and absence of external Na^+ . Despite a 40% block of current magnitude (see Fig. 5 A), addition of 100 mM Na^+ did not influence current activation or inactivation at 0 mV (Fig. 10 A; similar results were obtained with currents evoked by depolarization for 1.3 s, not shown). Similarly, current deactivation at -60 mV was unaffected by addition of 100 mM external Na^+ (Fig. 10 B). With 3 mM K^+ both internally and externally (and 140 mM internal, 160 mM external Tris), currents reversed at 0 mV with and without 100 mM external Na^+ present ($n = 3$; not shown), which demonstrates that Na^+ did not pass through the selectivity filter under these conditions. We conclude from these data that

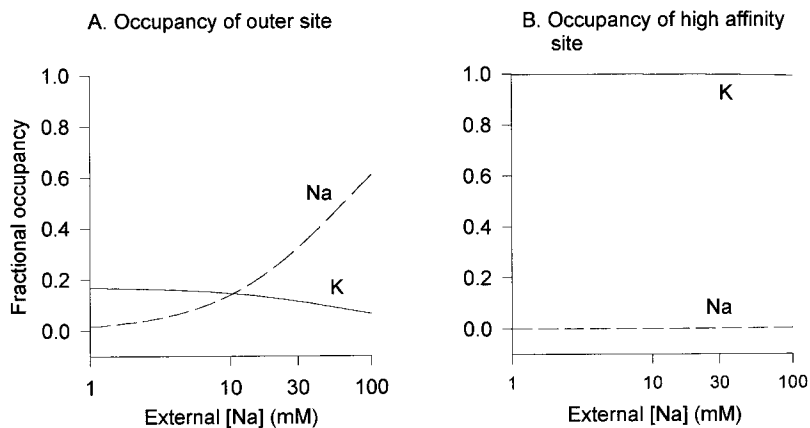


FIGURE 8. Predicted binding site occupancy with 3 mM external K^+ and increasing external $[Na^+]$. Model parameters from Fig. 4 A were used, as in Fig. 7, except that voltage was set to the experimentally used repolarization potential of -60 mV to maximize the possibility that Na^+ would reach the high affinity site. (A) Fractional occupancy of the outer, low affinity site by Na^+ and K^+ . (B) Fractional occupancy of the central, high affinity site by Na^+ and K^+ .

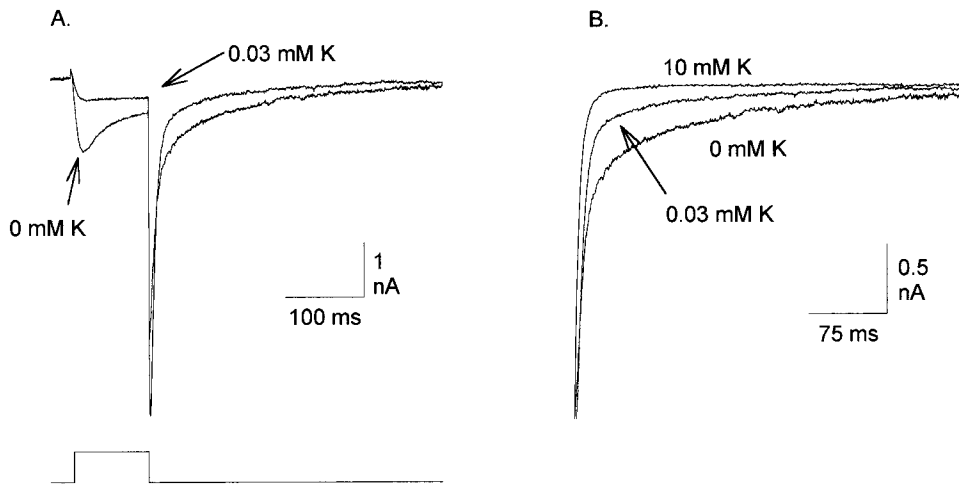


FIGURE 9. Effect of external K^+ on Na^+ current inactivation and deactivation. (A) Experimental procedure was identical to that of Fig. 3 (different cell). Currents in the absence of K^+ and in the presence of 0.03 mM K^+ were evoked by a 100 -ms depolarization to 0 mV. (B) Three tail currents from the cell in A, normalized at the current measured 210 μ s after repolarization and plotted on an expanded scale. Currents were recorded at -80 mV in the presence of 0 , 0.03 , and 10 mM K^+ .

(a) Na^+ did not displace K^+ from the high affinity binding site, (b) Na^+ did not block K^+ currents at the selectivity filter binding site, and (c) the cation-dependent effects on channel gating do not occur at the outer, low affinity binding site. These results are consistent with the predictions of the model.

DISCUSSION

In the delayed rectifier K^+ channel, Kv2.1, Na^+ , Li^+ , and Cs^+ all permeate in the absence of K^+ and permeation by these ions is competitively inhibited by K^+ (Korn and Ikeda, 1995; Immke, D., L. Kiss, J. LoTurco, and S.J. Korn, manuscript in preparation). This observation suggested that, like Ca^{2+} channels, selectivity in K^+ channels may at least partially result from differential affinity of different cations for an intrapore binding site. Unlike Ca^{2+} channels, however, K^+ did not appear to bind to

Kv2.1 with particularly high affinity. Indeed, the IC_{50} for block of Na^+ currents by K^+ was ~ 0.4 mM (data not shown), reflecting an affinity almost $1,000$ -fold lower than that of Ca^{2+} for the Ca^{2+} channel (Lansman et al., 1986).

We subsequently discovered that a chimeric K^+ channel, derived from Kv2.1 and Kv1.3, also conducted Na^+ in the absence of K^+ (Fig. 2; this channel also conducts Cs^+ and Li^+ in the absence of K^+ ; not shown). As in Kv2.1, the chimera displayed anomalous mole fraction behavior: low $[K^+]$ blocked Na^+ conductance and higher $[K^+]$ generated K^+ currents (Fig. 3). The chimera displayed an apparent affinity for K^+ of 0.03 mM or lower (Fig. 3 B). This high affinity block in a high flux channel suggested to us that K^+ channels may use much the same selectivity mechanism as Ca^{2+} channels.

Heginbotham et al. (1994) demonstrated that single amino acid substitutions in a conserved region of the K^+ channel pore (the signature sequence) could com-

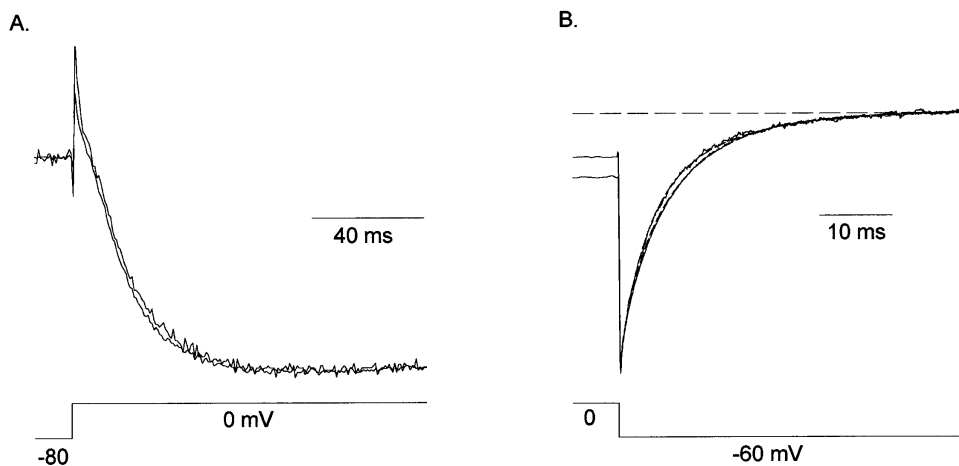


FIGURE 10. Effect of external Na^+ on K^+ current activation, inactivation, and deactivation kinetics. These currents, carried by 3 mM external K^+ , were obtained in experiments as described in Fig. 5. (A) Two normalized traces are superimposed, one obtained in the absence of external Na^+ , one obtained in the presence of 100 mM external Na^+ . In this cell, 100 mM Na^+ blocked the K^+ current by 42% at 0 mV. The activation time course for both currents was well-fit by a single exponential function, with time constants of 16.84 ± 1.87 and 18.50 ± 2.25 ms, in the absence and presence of Na^+ , respectively

($n = 5$). (B) Two normalized tail currents (solid lines) are superimposed, recorded in the absence and presence of Na^+ . Also superimposed on these currents are double exponential fits (dashed lines), which yielded identical fast and slow time constants under the two conditions ($\tau_1 = 5.98 \pm 0.43$ and 4.81 ± 0.62 ms, respectively; $\tau_2 = 2.49 \pm 0.56$ and 1.29 ± 0.49 ms, respectively; $n = 5$). In this cell, 100 mM Na^+ blocked the tail current by 49% . The horizontal dashed line represents the 0 current baseline.

pletely abolish ionic selectivity. These studies, together with molecular studies that suggest the presence of just a very short narrow region of the pore (see Goldstein, 1996), are consistent with the presence of just a single selective binding site in K^+ channels. In this study, we sought to determine whether we could explain the salient features of K^+ channel permeation behavior with a single, high affinity binding site hypothesis.

The main finding of this study is that permeation properties in at least two K^+ channels can be produced by a permeation pathway that contains a single high affinity binding site, flanked by low affinity binding sites, all of which have fixed affinities regardless of channel occupancy. The properties that we examined, and which the hypothesis predicts with reasonable quantitative accuracy, are anomalous mole fraction behavior between K^+ and Na^+ , linear current-voltage relationships, relative K^+ and Na^+ conductances, and low affinity block of K^+ currents by external Na^+ .

What Is Unique about this Model of the Permeation Pathway?

The most important conceptual difference between this model and all previous models of the permeation pathway is the hypothesis that there is only a single high affinity binding site in the pore and that there is only a single site of selectivity between K^+ and other cations. Furthermore, although electrostatic repulsion is not excluded by this model, this hypothesis proposes that the affinity of this site need not change with channel occupancy to account for K^+ channel permeation characteristics.

A necessary component of this hypothesis is that there are low affinity sites flanking the high affinity site. As with the high affinity site, these also need not change affinity with channel occupancy. This type of model could explain a variety of differences among K^+ channels with very subtle differences in amino acid architecture. For example, subtle alterations in the flanking low affinity sites could change single channel conductance or block by competing ions (i.e., Na^+) without altering the selectivity filter. Indeed, mutations have been made in K^+ channels that produce just such an effect (Kirsch et al., 1992; Zuhlke et al., 1994). Similarly, the ability of Na^+ to permeate the channel could be influenced by very subtle changes in just the selectivity filter binding site, perhaps with little influence on other channel properties. In the extreme, a change in few amino acids could convert a K^+ -selective channel into a nonselective cation channel (see Heginbotham et al., 1992) and vice versa.

Is Such a Model Biophysically Plausible?

Hille and Schwarz (1978) concluded that large flux ratio values, similar to those obtained from squid axon K^+ channels and *Shaker* K^+ channels (Hodgkin and

Keynes, 1955; Begenesich and DeWeer, 1980; Stampe and Begenesich, 1996), require large outer energy barriers (the energy required to enter and exit the pore) relative to inner barriers, and rapid mobility between binding sites within the pore (a function of low inner barriers). Despite having a single high affinity binding site within the pore, the model presented here fulfills this requirement. Arguments have been made that putting two to three ions in the pore likely results in electrostatic repulsion between ions (Hille and Schwarz, 1978; Levitt, 1986; Neyton and Miller, 1988; Stampe and Begenesich, 1996). However, these models assume that most or all of the ions in the pore reside in a narrow region of the pore. Molecular studies argue against this physical picture, however, and suggest that the narrow region of the pore may be as short as ~ 10 Å (see Goldstein, 1996; Miller, 1996). Conceptually, the model of the permeation pathway presented here, and the emerging model of channel architecture, are consistent with the ion fitting closely with the walls of the pore only over this short span. The low affinity binding sites, which by definition would be in wider "vestibules," may be electrically shielded from the ion at the selectivity filter. Neither experimental data nor the concepts in this model rule out the possibility that electrostatic repulsion occurs in multiply occupied pores. However, the model does show that high flux rates through a multi-ion channel with high affinity for the permeant ion do not require electrostatic repulsion (see also Dang and McCleskey, 1998).

Implications of the Model

This hypothesis raises two key issues. First, it proposes a novel mechanism by which multi-ion pores may produce high flux rates and yet be highly selective. Both Ca^{2+} channels and K^+ channels are multi-ion pores that have a high degree of selectivity and high flux rates, yet classical theories about the permeation mechanisms in these two channel types differed greatly. The data presented here and in Dang and McCleskey (1998) suggest that a single fundamental mechanism may be used by both channel types. It is intriguing, in this respect, that Na^+ channels also appear to have a single site of selectivity, and that both Na^+ and Ca^{2+} channels can be easily modified to select for other ions (Heinemann et al., 1992; Favre et al., 1996). Furthermore, this hypothesis suggests that modification of ion selectivity in ion channels may be generally accomplished with rather subtle modifications. Second, this hypothesis makes predictions about pore-dependent channel functions that are testable. It predicts, for example, that functional properties of different sites in the permeation pathway operate independently of the degree of channel occupancy. However, even if repulsion does play a role in permeation, the model predicts

that the channel contains binding sites of different affinity that allows for regulation of different pore functions at different ion concentrations.

Predictions of the Model

Just as with the Ca^{2+} channel, it is not known whether the multiple binding sites in the pore are structurally linked or independent. However, the data in Figs. 9 and 10 suggest that these binding sites are functionally separable. For example, binding of K^+ in the pore decreases the rate of slow inactivation (see Fig. 9 A; Lopez-Barneo et al., 1993; Baukrowitz and Yellen, 1996) and alters the rate of deactivation (see Fig. 9 B; Matteson and Swenson, 1986; Domo and Yellen, 1992; Korn and Ikeda, 1995). The low concentration of K^+ required to influence the rate of inactivation and deactivation suggests that the K^+ dependence of these functions results from interaction at the high affinity bind-

ing site. In contrast, physiological concentrations of Na^+ block currents carried by 3 mM K^+ by as much as 40% at 0 mV (Fig. 5) but do not change inactivation or deactivation kinetics (Fig. 10). This is consistent with the model prediction that Na^+ blocks at an outer, low affinity binding site and does not gain access to the high affinity binding site (Figs. 7 and 8). Since this model predicts that there is just one high affinity site at which these functional influences occur, and this site is presumably at the selectivity filter, the model further suggests that the influence of K^+ on gating kinetics results from its binding to the selectivity filter. Liu et al. (1996) suggested that C-type inactivation involves a constriction near the outer mouth of the pore. Together with the observation that K^+ binding within the pore slows inactivation, the hypothesis put forward by this model suggests that this constriction involves the selectivity filter.

We thank Dr. Ed McCleskey for enlightening discussions, a preprint of his paper, and for generously sharing his computer program. Thanks also to Dr. Rod MacKinnon for the chimera used in this study.

This work was supported in part by the National Science Foundation and the University of Connecticut Research Foundation.

Original version received 25 August 1997 and accepted version received 3 November 1997.

REFERENCES

- Almers, W., E.W. McCleskey, and P.T. Palade. 1984. A non-selective cation conductance in frog muscle membrane blocked by micromolar external calcium ions. *J. Physiol. (Camb.)* 353:565–583.
- Armstrong, C.M. 1989. Reflections on selectivity. In *Membrane Transport*. D.C. Tosteson, editor. American Physiological Society, Bethesda, MD. 261–274.
- Baukrowitz, T., and G. Yellen. 1996. Use-dependent blockers and exit rate of the last ion from the multi-ion pore of a K^+ channel. *Science* 271:653–656.
- Begenisich, T., and C. Smith. 1984. Multi-ion nature of potassium channels in squid axons. *Curr. Top. Membr. Trans.* 22:353–369.
- Bezanilla, F., and C.M. Armstrong. 1972. Negative conductance caused by entry of sodium and cesium ions into the potassium channels of squid axons. *J. Gen. Physiol.* 50:553–575.
- Dang, T., and E.W. McCleskey. 1996. A Ca^{2+} channel model without ionic interaction. *Biophys. J.* 70:A184.
- Dang, T., and E.W. McCleskey. 1998. Ion channel selectivity through stepwise changes in binding affinity. *J. Gen. Physiol.* 111:185–193.
- Domo, S.D., and G. Yellen. 1992. Ion effects on gating of the Ca^{2+} -activated K^+ channel correlate with occupancy of the pore. *Biophys. J.* 61:639–648.
- Ellinor, P.T., J. Yang, W.A. Sather, J.-F. Zhang, and R.W. Tsien. 1995. Ca^{2+} channel selectivity at a single locus for high-affinity Ca^{2+} interactions. *Neuron* 15:1121–1132.
- Favre, I., E. Moczydlowski, and L. Schild. 1996. On the structural basis for ionic selectivity among Na^+ , K^+ and Ca^{2+} in voltage-gated sodium channel. *Biophys. J.* 71:3110–3125.
- French, R.J., and J.J. Shoukimas. 1985. An ion's view of the potassium channel. The structure of the permeation pathway as sensed by a variety of blocking ions. *J. Gen. Physiol.* 85:669–698.
- French, R.J., and J.B. Wells. 1977. Sodium ions as blocking agents and charge carriers in the potassium channel of the squid axon. *J. Gen. Physiol.* 70:707–724.
- Goldstein, S.A.N. 1996. A structural vignette common to voltage sensors and conduction pores: canaliculi. *Neuron* 16:717–722.
- Gross, A., T. Abramson, and R. MacKinnon. 1994. Transfer of the scorpion toxin receptor to an insensitive potassium channel. *Neuron* 13:961–966.
- Hamill, O.P., A. Marty, E. Neher, B. Sakmann, and F.J. Sigworth. 1981. Improved patch-clamp techniques for high-resolution current recording from cells and cell-free membrane patches. *Pflügers Archiv* 381:85–100.
- Heginbotham, L., Z. Lu, T. Abramson, and R. MacKinnon. 1994. Mutations in the K^+ channel signature sequence. *Biophys. J.* 66:1061–1067.
- Heginbotham, L., T. Abramson, and R. MacKinnon. 1992. A functional connection between the pores of distantly related ion channels as revealed by mutant K^+ channels. *Science* 258:1152–1155.
- Heinemann, S.H., H. Terlau, W. Stuhmer, K. Imoto, and S. Numa. 1992. Calcium channel characteristics conferred on the sodium channel by single mutations. *Nature* 356:441–443.
- Hess, P., and R.W. Tsien. 1984. Mechanism of ion permeation through calcium channels. *Nature* 309:453–456.
- Hidalgo, P., and R. MacKinnon. 1995. Revealing the architecture of a K^+ channel pore through mutant cycles with a peptide inhibitor. *Science* 268:307–310.
- Hille, B. 1992. *Ionic channels in excitable membranes*. 2nd ed. Sinauer Associates Inc. Sunderland, MA.
- Hille, B., and W. Schwarz. 1978. Potassium channels as multi-ion single-file pores. *J. Gen. Physiol.* 72:409–442.

- Hille, B. 1973. Potassium channels in myelinated nerve. Selective permeability to small cations. *J. Gen. Physiol.* 61:669–686.
- Hodgkin, A.L., and R.D. Keynes. 1955. The potassium permeability of a giant nerve fibre. *J. Physiol. (Camb.)*. 128:61–88.
- Holmgren, M., P.L. Smith, and G. Yellen. 1997. Trapping of organic blockers by closing of voltage-dependent K⁺ channels. *J. Gen. Physiol.* 109:527–535.
- Jurman, M.E., L.M. Boland, Y. Liu, and G. Yellen. 1994. Visual identification of individual transfected cells for electrophysiology using antibody-coated beads. *Biotechniques*. 17:876–881.
- Kim, M.-S., T. Mori, L.-X. Sun, K. Imoto, and Y. Mori. 1993. Structural determinants of ion selectivity in brain calcium channel. *FEBS Lett.* 318:145–148.
- Kirsch, G.E., J.A. Drewe, H.A. Hartmann, M. Tagliatela, M. de Biasi, A.M. Brown, and R.H. Joho. 1992. Differences between the deep pores of K⁺ channels determined by an interacting pair of nonpolar amino acids. *Neuron*. 8:499–505.
- Korn, S.J., and S.R. Ikeda. 1995. Permeation selectivity by competition in a delayed rectifier potassium channel. *Science*. 269:410–412.
- Kuo, C.-C., and P. Hess. 1993. Characterization of the high-affinity Ca²⁺ binding sites in the L-type Ca²⁺ channel pore in rat pheochromocytoma cells. *J. Physiol. (Camb.)*. 466:657–682.
- Lansman, J.B., P. Hess, and R.W. Tsien. 1986. Blockade of current through single calcium channels by Cd²⁺, Mg²⁺, and Ca²⁺: voltage and concentration dependence of calcium entry into the pore. *J. Gen. Physiol.* 88:321–347.
- Levitt, D.G. 1986. Interpretation of biological ion channel flux data: reaction rate versus continuum theory. *Annu. Rev. Biophys. Chem.* 15:29–57.
- Liu, Y., M.E. Jurman, and G. Yellen. 1996. Dynamic rearrangement of the outer mouth of a K⁺ channel during gating. *Neuron*. 16: 859–867.
- Lopez-Barneo, J., T. Hoshi, S.H. Heinemann, and R.W. Aldrich. 1993. Effects of external cations and mutations in the pore region on C-type inactivation of *Shaker* potassium channels. *Receptors Channels*. 1:61–71.
- Matteson, D.R., and R.P. Swenson, Jr. 1986. External monovalent cations that impede the closing of K channels. *J. Gen. Physiol.* 87: 795–816.
- Miller, C. 1996. The long pore gets molecular. *J. Gen. Physiol.* 107: 445–447.
- Neyton, J., and C. Miller. 1988. Discrete Ba²⁺ block as a probe of ion occupancy and pore structure in the high conductance Ca²⁺-activated K⁺ channel. *J. Gen. Physiol.* 92:569–586.
- Perez-Cornejo, P., and T. Begenisich. 1994. The multi-ion nature of the pore in *Shaker* K⁺ channels. *Biophys. J.* 66:1929–1938.
- Polo-Parada, L., and S.J. Korn. 1997. Block of N-type calcium channels in chick sensory neurons by external sodium. *J. Gen. Physiol.* 109:693–702.
- Ranganathan, R., J.H. Lewis, and R. MacKinnon. 1996. Spatial localization of the K⁺ channel selectivity filter by mutant cycle-based structure analysis. *Neuron*. 16:131–139.
- Schumaker, M.F., and R. MacKinnon. 1990. A simple model for multi-ion permeation. Single-vacancy conduction in a simple pore model. *Biophys. J.* 58:975–984.
- Stampe, P., and T. Begenisich. 1996. Unidirectional K⁺ fluxes through recombinant *Shaker* potassium channels expressed in single *Xenopus* Oocytes. *J. Gen. Physiol.* 107:449–457.
- Yang, J., P.T. Ellinor, W.A. Sather, J.-F. Zhang, and R.W. Tsien. 1993. Molecular determinants of Ca²⁺ channel selectivity and ion permeation in L-type Ca²⁺ channels. *Nature*. 366:158–161.
- Yellen, G. 1984. Relief of Na⁺ block of Ca²⁺-activated K⁺ channels by external cations. *J. Gen. Physiol.* 84:187–199.
- Zuhlke, R.D., H.-J. Zhang, and R.H. Joho. 1994. Role of an invariant cysteine in gating and ion permeation of the voltage-sensitive K⁺ channel Kv2.1. *Receptors Channels*. 2:237–248.